Tectonics in the Eastern Asia inferred from GPS observations

Shin'ichi MIYAZAKI, Shigeru MATSUZAKA, Kosuke HEKI,[1] Masaru KAIDZU, Yuki KUROISHI, Masaki MURAKAMI, Tetsuro IMAKIIRE, Takashi TADA, Koh NITTA, Hiroyuki NAKAGAWA, Akifusa ITABASHI, Masao KARASAWA, Osamu OOTAKI, Norihiko ISHIKAWA, Masayoshi ISHIMOTO, Hiroaki TAKAHASHI,[2] Minoru KASAHARA[2], and Ki-Dok An[3]

Abstract

The crustal velocity field in Eastern Asia is investigated. We first analyze continuous GPS data for Korea,Far East Russia,China, and southwest Japan.Velocities are found to have an apparent eastward component relative to the stable interior of the Eurasian plate,and this eastward motion is fairly rigid in the region that includes Suwon,and Taejon (Korea),Xian (China),and Vladivostok and Yuzhno-Sakhalinsk (Russia). This area corresponds to the Amurian plate and its Euler vector with respect to the Eurasian plate is estimated to be (21.7°,108.0°, - 0.092° /Ma). This result predicts that the convergence rate at the eastern margin of the Sea of Japan is about 16 ~ 18 mm/yr as the Amurian - North American relative plate motion. The result also implies that the convergence rate at the Nankai Trough is 60 ~ 65 mm/yr and the resultant deformation by this plate interaction reaches the northernmost part of the Chugoku district. The crustal velocity field of southwest Japan relative to the Amurian plate gives its intraplate deformation. We show that the obtained velocity field could be decomposed into an elastic loading by subduction and a collision-related deformation.

1 Introduction

Spreading rates at mid-oceanic ridges, strikes of transform faults,and slip vectors of interplate earthquakes have been used to model the movements of tectonic plates in terms of Euler vectors [e.g., *DeMets et al.*, 1990]. However, all these data are derived along plate boundaries, so it is important that we know the exact plate boundaries in advance. When we study the movement of a plate with diffuse boundaries, velocities of space geodetic stations obtained by repeated site occupations are more suitable, that is, all we need to know is that the sites reside on the stable interior of the plate in concern.

Recent global space geodetic measurements have demonstrated that the velocities of tectonic plates originally modeled for the last few millions of years also hold for time scales as short as a decade. *Heki* [1996] established a three-dimensional Very Long Baseline Interferometry (VLBI) kinematic reference frame by minimizing the difference between the velocities of stable plate interior stations and those predicted by nnr-NUVEL1a [*Argus and Gordon*, 1991, *DeMets et al.*, 1994]. He also estimated the velocities of sites close to plate boundaries relative to the plates on which the sites are supposed to reside. In Japan, the velocity of Tsukuba relative to the Eurasian plate (EU) appears to be about 20.5*mm/yr* toward the west and 2.7*mm/yr* toward the north. These values have been used as the reference velocities to relate local and regional velocity fields in and around Japan to a global plate tectonic framework.

Further, the recent expansion of IGS network allows us to extract plate motions in more detail. Several organizations routinely produce GPS site velocity fields in ITRF reference frames for all of IGS sites, the number of which has now surpassed 100. Among the products, data from JPL is available on the world wide web [*Heflin*, 1998]. Figure 1 shows some JPL products which we transformed into ones relative to the Eurasian plate, supposing that the kinematic part of ITRF coincides with nnr-NUVEL1a. Once site velocities are obtained relative to the stable interior of a certain plate, we can estimate the Euler vector for relative plate motions or absolute motions

1) Division of Earth Rotation, National Astronomical Observatory, Mizusawa, Japan.
2) Institute of Seismology and Volcanology, Graduate School of Science, Hokkaido University, Sapporo, Japan.
3) National Geography Institute, Suwon, Kyonggi, Korea.

This document is provided by JAXA.

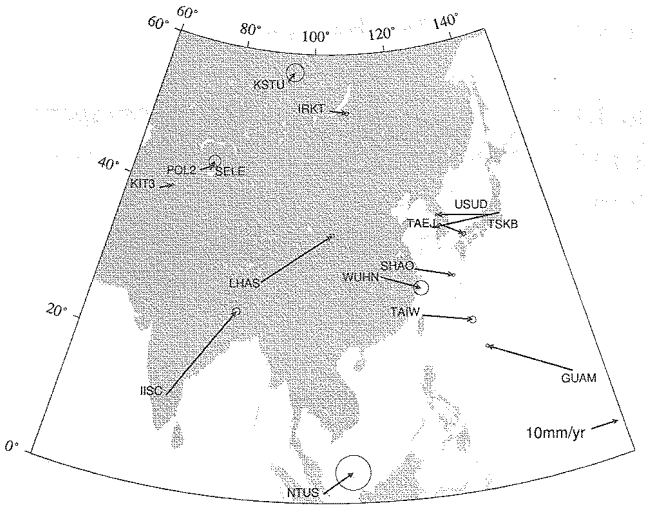

Figure 1. Global plate motion relative to the Eurasian plate deduced from IGS global network. (modified from Heflin [1998])

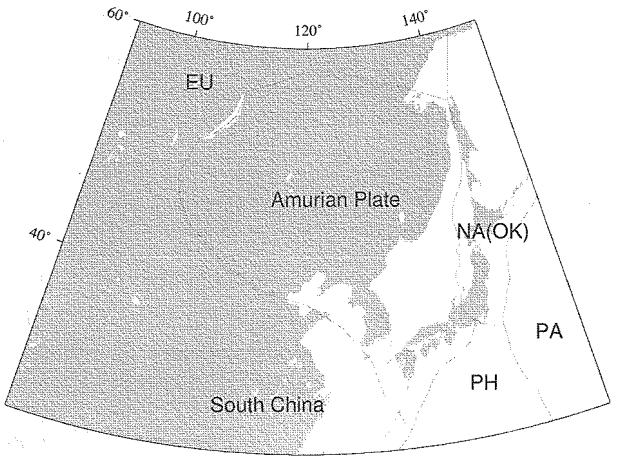

Figure 2. Plate setting in eastern Asia. EU stands for Eurasian plate, PH for Philippine Sea plate, NA for North American plate, PA for Pacific plate.

by assuming an absolute frame such as no-net-rotation frame.

The majority of the present study was conducted as a part of the "Assessment of the potential of earthquake occurrence at the eastern margin of the Sea of Japan", supported by the Science and Technology Agency. The essense of the present paper is also found in *Heki et al.* [1999].

2 The Amurian plate and its motion

Zonenshain and Savostin [1981] hypothesized the existence of the Amurian plate (AM) covering eastern Mongolia, northeastern China, southeastern Siberia and the Korean peninsula (Figure 2). It is supposed to move eastward as one of the consequences of the lateral expulsion of crustal blocks caused by the Indian collision into Eurasia [*Molnar and Tapponnier*, 1975]. Recently *Ishibashi* [1995] suggested that this eastward motion generates the east-west compression of the inner arc of the southwest Japan arc as manifested by the 17 Jan 1995 Hyogoken Nanbu earthquake [*Hashimoto et al.*, 1996]. It is therefore important to determine the plate motion of the Amurian plate for long-term hazard assessment in Japan as well as for tectonics studies.

Zonenshain and Savostin [1981] suggested that the northern and eastern boundaries of the Amurian plate run from the Baikal Rift to northern Sakhalin through the Stanovoi Range. Its southern boundary, however, remains ambiguous; it could lie along the Nankai Trough [*Wei and Seno*, 1998] or the Median Tectonic Line [*Tamaki and Honza*, 1985]. *Wei and Seno* [1998] estimated the Eular vector of AM relative to EU using earthquake slip vectors by assuming their southern boundary as the Nankai Trough. They employed a six-plate model, which consists of AM, EU, the Okhotsk (OK), the Philippine Sea (PH), the Pacific (PA), and the North American (NA) plate, and examined the focal mechanisms of earthquakes occurring between 1977 and 1995, to obtain 5 transform fault azimuths and 13 slip vectors in the Lake Baikal and Stanovoi Range regions relating to the AM-EU boundary, in addition to 364 slip vectors for other regions. Combining these data with 25 spreading rates, they computed all the closure-enforced Euler vectors simultaneously using the Monte-Carlo box method. They estimated the Euler vector for AM-EU as (60.42°N, 123.25°E, 0.025°/*m.y.*), which implies an extension rate along the Baikal Rift of 0.4 ~ 0.7*mm/yr*. According to their AM-OK Euler vector, the convergence rate along the eastern margin of the Sea of Japan amounts to 6 to 15*mm/yr*.

Miyazaki et al. [1996] also estimated AM-EU Euler vector using the GPS site velocities of Suwon in South Korea and several GEONET sites located in the northernmost part of the Japanese island of Chugoku. All of the sites are situated within AM, though we do not exactly know where its southern boundary is. However,

This document is provided by JAXA.

GPS sites are located in a small area in comparison with the whole Amurian plate. To improve this spatially biased distribution of GPS sites, they made use of the slip vectors of 13 earthquakes that had occurred along the northwestern boundary of the plate given by *Wei and Seno* [1998]. Euler vector estimated by *Miyazaki et al.* [1996] is (65.5°N, 131.4°E, 0.427°/*m.y.*), which gives a larger convergence rate of 2*cm/yr* along the eastern margin of the Sea of Japan than predicted from the relative motion of AM-NA by *Wei and Seno* [1998]. They further suggested

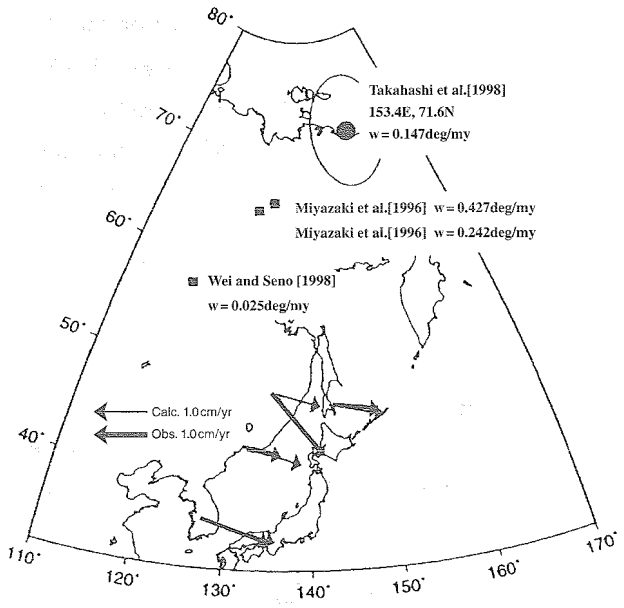

Figure 3. Estimated Euler pole of the Amurian plate. (modified from Takahashi et al. [1999])

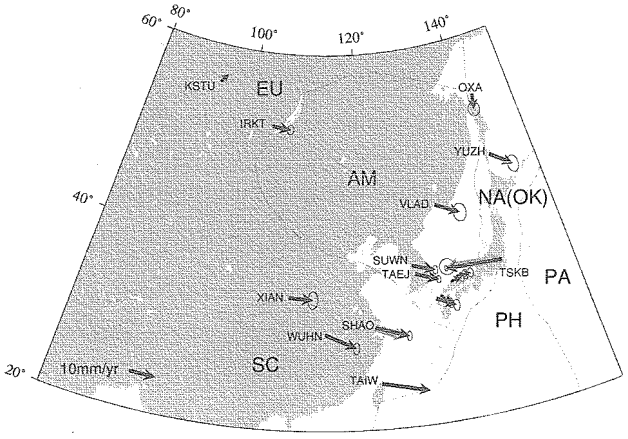

Figure 4. Site velocities of GPS stations used in this study. Error ellipses represent 1σ. Black arrows show GPS velocity; gray arrows at TSKB and SHAO show VLBI velocity; blue arrows show the results of Heflin [1998]

from their analysis that OK was not necessary to introduce. After the study of *Miyazaki et al.* [1996] several GPS sites were installed in South Korea, China, and Russia. *Takahashi et al.* [1999] chose Taejon (TAEJ) of South Korea from IGS stations, Vladivostok (VLAD) of Russia from the Western Pacific Integrated Network of GPS (WING) [*Kato et al.*, 1998b], and their own sites at Yuzhno-Sakhalinsk (YUZH) and Khabarovsk (KHAB) in Russia. They analyzed the data with Bernese software to estimate the Euler vector of AM-EU at (71.6°N, 153.4°E, 0.147°/*m.y.*)(Figure 3). However, it is difficult to confirm from their results the existence of AM because the residuals of site velocities at KHAB and VLAD were in the order of 5.0 to 10.0 *mm/yr*.

In order to demonstrate the existence of AM, it is necessary to show that the plate moves as a rigid body. In this paper, we reprocess the GPS data of several sites that are considered to be on AM together with those of surrounding sites in China and Japan.

3 Data and analysis

Data from several GPS points in Eastern Asia were used, as shown in Figure 4. In Korea, the National Geographical Institute has been operating a GPS station at Suwon. The station was registered as an IGS station on November 30, 1997. We also use the GPS data of four IGS stations, XIAN, SHAO, WUHN in China, and TAEJ in Korea. In Russia, in addition to IGS points such as Irkutsuk (IRKT), GPS data are available for VLAD [*Kato et al.*, 1998b] as well as for Okha (OXA) and YUZH, Sakhalin, operated by Hokkaido University and the Institute of Marine Geology of the Russian Academy of Science [*Takahashi et al.*, 1999]. We further make use of the data of five GEONET stations in northern Kyushu and the Chugoku district, Southwest Japan. Data from the Tsukuba IGS station (TSKB) are also analyzed in order to compare the GPS results with VLBI results.

Among these stations, SUWN, TAEJ, and VLAD are considered to be on the stable interior of AM. IRKT is located on the western flank of the Baikal Rift, just beyond the boundary with EU. SHAO and WUHN are located in the South China block being extruded eastward slightly faster than 1*cm/yr* [*Holt et al.*, 1995; *Peltzer and*

This document is provided by JAXA.

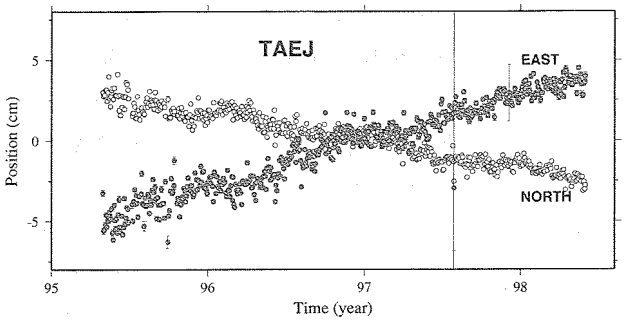

Figure 5. Time series of horizontal position of TAEJ.

Saucier, 1996], and XIAN is just north of the Qinling fault that is considered to divide the North China and South China blocks [*Peltzer et al.*, 1985]. Because of the ambiguity of AM-NA boundary, it is not clear whether OXA and YUZH lie on AM or on NA. Five GEONET sites are located on AM, and TSKB is on NA, though the motions of these sites are likely to be affected by the crustal deformation due to the subducting motions of PH and PA.

GPS data are analyzed by the strategy described in the following manner. We employ the Precise Point Positioning (PPP) technique available in GIPSY software with fiducial-free orbit and clock information, and correct the GPS data for the effect of atmospheric gradient to reduce the scatter and error of site coordinates and of site velocities.

Figure 5 shows the time series of horizontal position of TAEJ. From such time series as given in the figure, we estimate site velocities in ITRF96.

Since the kinematic part of ITRF96 is adjusted to that of the nnr-NUVEL1a plate motion model [*Argus and Gordon*, 1991; *DeMets et al.*, 1994], the site velocities obtained in ITRF96 can be converted to those relative to the stable part of EU by subtracting the absolute motion of EU. In other words, if a site is located just on the stable Eurasian plate, its site velocity relative to EU should be zero. The site velocities of TSKB and SHAO estimated from GPS data are compared with the velocities of corresponding Tsukuba and Shanghai VLBI points obtained by *Heki* [1996]. The GPS velocities coincide well with the VLBI velocities within the uncertainty of σ (Figure 4). The obtained velocities are listed in Table 1.

4 Observation equation

The GPS site velocities listed in Table 1 show that VLAD, SUWN, TAEJ, which are considered to belong to

Name	Station		Period		Velocity (mm/yr)		Error (mm/yr)		Plate
	Lat(°)	Lon(°)	From	To	North	East	North	East	
SUWN	37.3	127.1	95Apr30	98Jun09	-2.7	8.4	0.4	0.7	AM
TAEJ	36.4	127.4	95Apr30	98Jun09	-3.2	8.4	0.4	0.6	AM
VLAD	43.2	131.9	96Feb09	97Oct02	-4.4	8.7	1.1	1.6	AM
XIAN	34.4	109.2	96Jul11	98Apr21	-0.5	9.1	0.9	1.5	? *4
YUZH	47.0	142.7	95Jul28	97Jul30	-6.0	7.4	0.9	1.4	? *4
0073 *1	35.5	133.7	95Jul17	98Jun09	0.0	4.0	0.5	0.8	AM
0074 *1	35.4	133.1	95Jul17	98Jun09	0.0	3.6	0.5	0.8	AM
0075 *1	35.0	132.2	95Jul17	98Jun09	0.8	4.3	0.5	0.8	AM
0087 *1	33.7	130.5	95Jul17	98Jun09	-3.5	3.4	0.5	0.9	AM
0091 *1	33.5	129.9	95Jul17	98Jun09	-3.6	7.1	0.6	1.0	AM
IRKT	52.2	104.3	95Oct13	98Jun09	-0.8	6.8	0.6	0.8	EU
OXA	53.6	142.9	95Jul25	97Aug15	-5.6	-1.0	1.0	1.2	? *4
SHAO	31.1	121.2	95Apr30	98Jun09	-3.9	12.3	0.4	0.8	SC
TSKB	36.1	140.1	95Apr30	98Jun09	2.2	-21.0	0.3	0.5	NA
WUHN	30.5	114.4	96Jan25	98Jun09	-5.2	11.8	0.5	1.0	SC
KSTU *2	56.0	92.8	-	-	3.5	2.3	1.1	1.1	EU
TAIW *2	25.0	121.5	-	-	-3.8	17.6	0.4	0.4	SC
Seshan25 *3	30.9	121.2	-	-	-4.2	10.3	1.2	1.2	SC
Tsukuba *3	35.9	140.1	-	-	2.7	-20.5	1.3	1.4	NA

Table 1. Velocities of GPS sites relative to the Eurasian plate.

*1 GEONET station, *2 results of Heflin [1998], *3 VLBI station, *4 Plate to which the station belongs is unknown.

This document is provided by JAXA.

AM, move coherently in an E to ESE direction without showing any appreciable relative velocity to one another. We treat these three sites as core sites for the least-squares estimation of the AM-EU Euler vector. However, these core sites are located in a smaller area than the whole Amurian plate. Since the plate boundary of AM is not well defined, we can consider three cases for the Euler pole estimation. XIAN and YUZH have negligibly small velocities relative to the core sites, which suggests that these sites are involved in AM. In the first case (1), therefore, we combine the core site velocities with these two site velocities. This strategy may be called space geodetic strategy. XIAN is in the Weihe graben at the southern tip of the so-called Ordos block, and we do not know if this block is a part of AM. Moreover, XIAN is only a few tens of kilometers north of the Qinling fault, the northern boundary of the South China block [*Zhang et al.*, 1995], and it is doubtful that XIAN velocity is free from the buildup of elastic strains between the two blocks. YUZH is considered to be the east of the AM-NA boundary, though no geological or seismological studies have ever allowed us to draw a clear boundary there.

In the second case (2), therefore, we exclude the data of XIAN and YUZH from the least squares estimation. On the other hand, it is physically reasonable to include, in addition to the core site velocity data, the velocity direction of IRKT by regarding it as representative of the plate interaction of AM-EU.

In the third case (3), we make use of the data of earthquake slip vectors in addition to the IRKT velocity direction. We include 13 slip vectors of earth-quakes that occurred along the northwestern boundary of the plate [*Wei and Seno*, 1998].

In general, site velocity v for site s is expressed by an Euler vector ω as

$$v_S = \omega \times r_S \tag{1}$$

where r_S is the position vector of site s. This can be rewritten as

$$\begin{aligned} v_S &= (\omega_2 r_{s3} - \omega_3 r_{s2}) e_1 + (\omega_3 r_{s1} - \omega_1 r_{s3}) e_2 + (\omega_1 r_{s2} - \omega_2 r_{s1}) e_3 \\ &= (r_{s2} e_3 - r_{s3} e_2)\omega_1 + (r_{s3} e_1 - r_{s1} e_3)\omega_2 + (r_{s1} e_2 - r_{s2} e_1)\omega_3 \end{aligned} \tag{2}$$

where e_1, e_2, e_3 are the basic vectors of Earth-centered and Earth-fixed Cartesian coordinates. We hereafter omit the suffix s. We suppose that the shape of the earth is spherical, and introduce the polar coordinates e_r, e_θ, e_ϕ through the relations

$$\begin{bmatrix} e_1 \\ e_2 \\ e_3 \end{bmatrix} = \begin{bmatrix} \cos\theta\cos\phi & -\sin\theta\cos\phi & -\sin\phi \\ \cos\theta\sin\phi & -\sin\theta\sin\phi & \cos\phi \\ \sin\theta & \cos\theta & 0 \end{bmatrix} \begin{bmatrix} e_r \\ e_\theta \\ e_\phi \end{bmatrix} \tag{3}$$

In the polar coordinates, v can be written as

$$v = v_{NS} e_\theta + v_{EW} e_\phi \tag{4}$$

or, equivalently,

$$\begin{cases} v_{NS} = (r_2\cos\theta + r_3\sin\theta\sin\phi)\omega_1 + (-r_3\sin\theta\cos\phi - r_1\cos\phi)\omega_2 \\ \qquad + (-r_1\sin\theta\sin\phi + r_2\sin\theta\cos\phi)\omega_3 \\ v_{EW} = (-r_3\cos\phi)\omega_1 + (-r_3\sin\phi)\omega_2 + (r_1\cos\phi + r_2\sin\phi)\omega_3 \end{cases} \tag{5}$$

Note that the radial component is ignored because the vertical motion is out of our interest. Rewriting equation (2) by making use of (3), we have observation equations for linear inversion:

$$\begin{bmatrix} v_{NS} \\ v_{EW} \end{bmatrix} = \begin{bmatrix} \frac{r_2\sqrt{r_1^2+r_2^2+r_3^2}}{\sqrt{r_1^2+r_2^2}} & -\frac{r_1\sqrt{r_1^2+r_2^2+r_3^2}}{\sqrt{r_1^2+r_2^2}} & 0 \\ -\frac{r_3 r_1}{\sqrt{r_1^2+r_2^2}} & -\frac{r_2 r_3}{\sqrt{r_1^2+r_2^2}} & \sqrt{r_1^2+r_2^2} \end{bmatrix} \begin{bmatrix} \omega_1 \\ \omega_2 \\ \omega_3 \end{bmatrix} \tag{6}$$

For the direction data of velocity and slip vectors, the observation equation is

$$\Theta v = \tan^{-1}\left(\frac{v_{NS}}{v_{EW}}\right) \tag{7}$$

Substituting (5) into the above equation, we get

$$\begin{aligned} \Theta v = \tan^{-1}\Bigg[& \frac{(r_2\cos\theta + r_3\sin\theta\sin\phi)\omega_1\,\omega_3}{(-r_3\cos\phi)\omega_1 + (-r_3\sin\phi)\omega_2 + (r_1\cos\phi + r_2\sin\phi)\omega_3} \\ & + \frac{(-r_3\sin\theta\cos\phi - r_1\cos\theta)\omega_2\,\omega_3}{(-r_3\cos\phi)\omega_1 + (-r_3\sin\phi)\omega_2 + (r_1\cos\phi + r_2\sin\phi)\omega_3} \\ & + \frac{(-r_1\sin\theta\sin\phi + r_2\sin\theta\cos\phi)\omega_3}{(-r_3\cos\phi)\omega_1 + (-r_3\sin\phi)\omega_2 + (r_1\cos\phi + r_2\sin\phi)\omega_3} \Bigg] \end{aligned} \tag{8}$$

This document is provided by JAXA.

We calculate the partial derivatives of Θ_v with respect to ω, and perform an iterative nonlinear least-squares method to estimate the AM-EU Euler vector in the cases of (2) and (3).

For the nonlinear cases of (2) and (3), we used the Euler vectors obtained for the linear case of (1) as the initial value of the nonlinear least-squares method. Based on the variance of data around the solution, the standard deviations of GPS site velocities can be estimated.

On the other hand, no standard deviations have generally been given for the slip directions of earthquakes. *Wei and Seno* [1998] assigned 15 or 20 degrees to the standard deviations of slip directions depending on the results of a certain kind of quality test for the moment tensor solutions. In the present study, we adopted the standard deviations of slip vectors used by *Wei and Seno* [1998].

5 Results

5. 1 Euler vector for the Amurian plate

The results are summarized in Table 2 and in Figure 6. Unlike the results of previous studies described in the preceding section, the pole position was estimated for all cases (1) ~ (3) on the southern hemisphere, which predicts a larger eastward velocity along the northern tip of AM than its southern part. In the case of (1), the Euler vector is estimated as (21.7°S, 108.0°E, -0.092°/*m.y.*) with the Euler pole displayed in Figure 6. The weighted root mean square (wrms) estimated for the observation of site velocities is as small as 0.33*mm/yr*, which suggests that the area that is presumed to be AM moves as a rigid body, and that the pole position is well constrained (case (1) in Figure 6).

For case (2), the estimated Euler vector is (50.2°S, 95.0°E, -0.081°/*m.y.*). The wrms of the postfit velocity residuals is 0.31*mm/yr*, and the direction residual of IRKT is 0.9°. The pole position is considered to be well constrained (case (2) in Figure 6).

Finally in case (3), the estimated Euler vector is (73.5°S, 40.4°E, -0.098°/*m.y.*). The wrms of the velocity residuals is 0.40*mm/yr*, and that of the direction residuals is 20.5°. The pole position is also considered to be well constrained (case (3) in Figure 6).

In the later discussion, we will examine the results of case (1). Even if we use the Euler vector of the other cases, the essential part of our discussion would hardly be changed because the predicted velocities of GPS sites

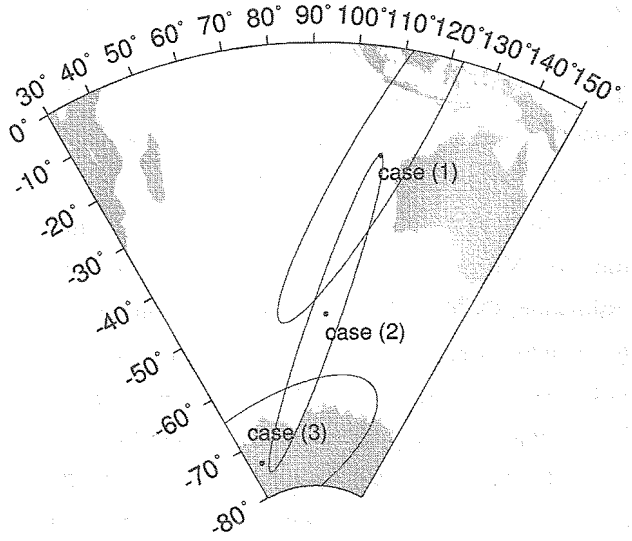

Figure 6. Euler pole between the Amurian and the Eurasian plates for cases (1) ~ (3). Error ellipses indicate 2σ.

Plate pair	Strategy	Pole		Angular Rate		Error Ellipse		
		Lat(°)	Lon(°)	ω(°/*Ma*)	σ_ω(°/*Ma*)	σ_{lat}(°)	σ_{lon}(°)	correlation
AM-EU	case(1)	21.7S	108.0E	-0.092	0.011	12.4	3.9	-0.91
AM-EU	case(2)	50.2S	95.0E	-0.081	0.004	13.9	6.0	-0.95
AM-EU	case(3)	73.5S	40.4E	-0.098	0.016	4.5	10.2	-0.34
AM-NA*1	-	78.3S	16.7E	0.029	-	-	-	-
AM-PH*2	-	46.8S	22.1W	1.365	-	-	-	-

Table 2. Estimated Euler vectors of the relative motion of the Amurian plate relative to the Eurasian plate.

*1 EU-NA pole of NUVEL1a [DeMets et al., 1994] was used.

*2 EU-PH pole of Kotake et al. [1998] was sed.

This document is provided by JAXA.

coincide with the observed ones within 2σ, where σ is the standard deviation for the observed data.

5. 2 Kinematics of the Amurian plate relative to its adjacent areas

Since there are few GPS stations in the Far Eastern region, it has been difficult to investigate the kinematics of this area. The Euler vector of AM obtained in this study is so reliable that we may discuss the kinematics of other adjacent tectonic blocks in order to confirm the necessity of its existence. There is one GPS station at Krasnoyarsk (KSTU) about 800*km* northwest of the AM-EU boundary. Figure 1 (modified from *Heflin* [1998]) includes the velocity of KSTU relative to EU. The site velocity of KSTU is 2.26 $\pm$ 1.07*mm/yr* to the east and 3.48 $\pm$ 1.07*mm/yr* to the north, which shows a significantly different direction from that expected for AM, although the velocity is less reliable than other sites because of its short observation period. This supports that AM is distinguishable from the rest of the EU.

WUHN and SHAO are considered to be on the South China block (SC), and have little mutual movement. The velocities of these stations are consistent with those derived from earthquake strain rates within central and eastern Asia by *Holt et al.* [1995]. A left-lateral strike slip movement is known to exist along the E-W striking Qinling fault [*Peltzer et al.*, 1985], and is considered to divide SC and the North China block. Our results are consistent with this long-term deformation.

Once the Euler vector of AM-EU is obtained, we can calculate Euler vectors for AM-NA and AM-PH. Since the Euler vector of EU-NA is given by NUVEL1a [*DeMets et al.*, 1994], we can obtain an AM-NA Euler vector by combining these two vectors of AM-EU and EU-NA. For the calculation of the AM-PH Euler vector, it does not seem appropriate to use the EU-PH Euler vector of *Seno et al.* [1993], because they assumed the slip vectors of earthquakes occurring along the Nankai Trough to be representative of the motion of EU-PH. *Kotake et al.* [1998] estimated EU-PH Euler vector by using GPS site velocities on PH in a similar way as in this study. Using their results, we calculate the AM-PH Euler vector. The Euler vectors are estimated to be (78.3°S, 16.7°E, 0.029°/*m.y.*) for AM-NA and (46.8°S, 22.1°W, 1.365°/*m.y.*) for AM-PH.

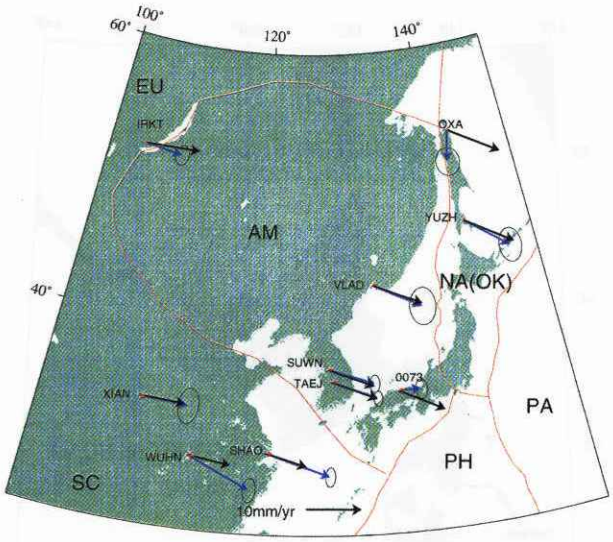

Figure 7. Comparison of predicted site velocity between the AM-EU pole reported here and that reported by Wei and Seno [1998] . Black arrows show the predicted velocities by our AM-EU pole; red arrows show the predicted velocities by Wei and Seno [1998]; blue arrows are observed velocities.

6 Discussion

6. 1 Baikal Rift and the Stanovoi Range

As stated before, the boundary of AM is generally diffused. The border between AM and EU, however, is best constrained along the Baikal Rift and Stanovoi Range. AM-EU Euler vector estimated in the present study suggests a nearly E-W extension along the Baikal Rift and a left-lateral strike-slip movement along the Stanovoi. *Wei and Seno* [1998] listed 13 earthquake slip vectors along the Baikal Rift and Stanovoi Range, and we may categorize them into two groups: nine of them with a NW-SE orientation and the remaining four showing a nearly E-W orientation. Our Euler vector is consistent only with the latter group.

Since the Euler vector of *Wei and Seno* [1998] was obtained by using slip vectors, it explains the slip vectors better than our Euler vector. However, their Euler vector does not satisfy the observed GPS site velocities of core sites; the site velocities expected of their Euler vector differ from the observed ones by 30° ~ 45° in azimuth and by one order of magnitude in length (Figure 7). It seems difficult to explain both the GPS site velocities and the

This document is provided by JAXA.

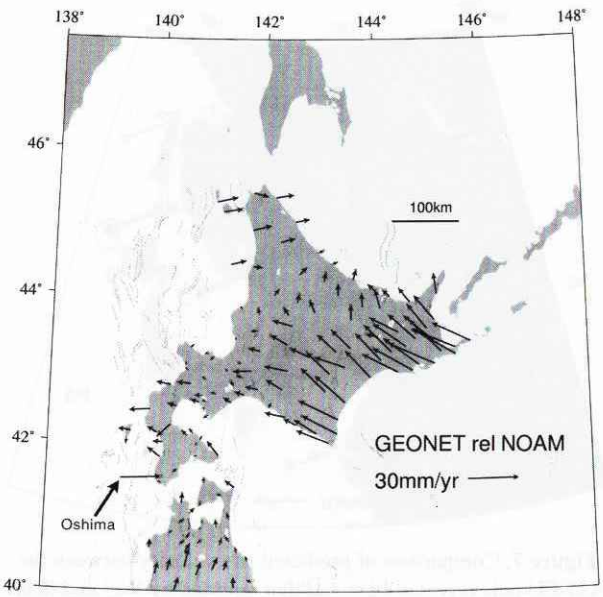

Figure 8. The velocity at Oshima-Ohshima island relative to the North American plate. Other velocities are taken from GEONET stations.

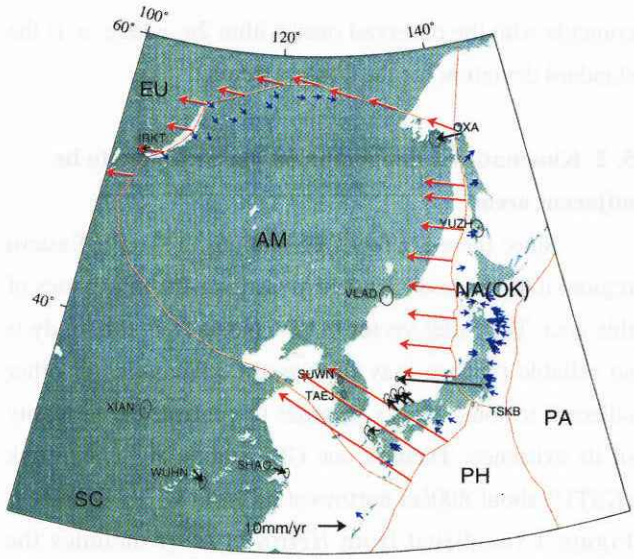

Figure 9. Earthquake slip vectors and predicted slip direction from AM-PH Euler vector. Blue arrows show slip vectors; black arrows show the observed velocity w. r. t. AM; red arrows show relative plate motion of adjacent plates with AM.

earthquake slip vectors by a single Euler pole. However, compared with the mutual coherency of the GPS site velocities, the directions of the slip vectors are rather scattered even along the Baikal Rift and Stanovoi Range. This suggests the existence of other tectonic forces to generate earthquakes, for example, the detachment of the Baikal region from AM. Further studies are needed to clarify the origin of this inconsistency.

6. 2 Eastern margin of the Japan Sea and Sakhalin

As shown in Figure 7, the observed velocity of YUZH is close to that predicted by our Euler vector. The velocity field of northern Hokkaido shows an eastward motion with a rate smaller than that of YUZH [*Miyazaki*, 1999]. This suggests that the AM-NA plate boundary in the region from Hokkaido to central Sakhalin runs somewhat east of the previously proposed one shown in Figure 4. As seen in Figure 7, the observed velocity of OXA is different both in direction and in magnitude from that expected for the Euler vector of AM-NA. This implies that OXA does not belong to AM and that its boundary runs somewhere west of OXA.

A campaign observation was conducted in the Oshima-Ohshima Island in Hokkaido in 1996 and 1999. We derived the velocity there by using the GPS data obtained in 1996 and 1999, and converted to that relative to NA. Although observation was conducted for 3 days in 1999, data from 1996 is limited to a single day; hence, it is likely that the obtained velocity (Figure 8) is not accurate enough to discuss the implication to the tectonics. If the results are accurate, they could suggest that the AM-NA boundary runs east of the Oshima-Oshima or the interplate coupling is almost full.

The convergence rate along the eastern margin of the Sea of Japan becomes 16 to 18*mm/yr*. Several large earthquakes with slips as large as 3*m* have recently occurred here, such as the 12 July 1993 Hokkaido-Nansei-Oki earthquake (M_W=7.8) and the 26 May 1983 Nihonkai-Chubu earthquake (M_W =7.7). Assuming that this is the characteristic size of interplate earthquakes like these and that the interplate coupling is 100%, the recurrence interval of characteristic earthquakes would be 200 years.

However, historic seismic activity studies suggest that this is not the case [*Seno et al.*, 1996]. One possible explanation is that the interplate coupling of this area is less than 100%, which makes the recurrence interval longer. If the recurrence interval of this region is longer than 300 years, the seismic coupling should be smaller than 60%.

This document is provided by JAXA.

6. 3 Nankai Trough

The slip vectors observed for earthquakes along the Nankai Trough are consistent in direction with those predicted by our AM-PH Euler vector, as demonstrated in Figure 9. *Seno et al.* [1993] presumed these slip vectors represented the EU-PH direction without considering the existence of AM. It is now necessary to revise PH Euler vectors by taking account of the AM movement. However, such revision would be minor, because the eastward movement of AM along the Nankai Trough is only about 1*cm/yr*, deflecting the EU-PH direction predicted by *Seno et al.* [1993] conterclockwise only by about 2°. This minor correction is much smaller than typical errors amounting to 15° of slip direction data.

Continuous GPS observations revealed northwestward motions at the southern tip of Shikoku Island. Assuming that the northwestward motions are caused by the coupling between EU and PH, several recent studies estimated the coupling strength by using the concept of backslip [e.g. *Ozawa et al.*, 1999]. It was found in this study, however, that the motion directions of three GEONET sites in the Chugoku district coincided with those expected not for EU-PH but for AM-PH motion, suggesting that the interplate coupling between AM and PH affects not only the outer arc but also the inner arc of southwest Japan. The state of plate coupling along the Nankai Trough should thus be recalculated on the basis of the kinematic reference frame fixed to AM.

6. 4 Implication for the velocity field of southwest Japan

So far the velocity field of the southwest Japan has been represented relative to the stable interior of EU [e.g. *Sagiya et al.*, 2000]. This reference frame could serve as a neutral one and may have some advantages when we discuss the crustal velocity field of Japan as a whole. However, if site velocities are obtained relative to its belonging plate, it is possible to interpret them as the intraplate deformation. We demonstrated that southwest and northeast Japan are affliated with AM and NA, respectively. Hence it seems appropriate to express the crustal velocities of southwest and northeast Japan relative to AM and NA, respectively. In the present paper, we briefly examine the features that are observed in the velocity field of southwest Japan relative to AM. More detailed discussions are found in *Miyazaki and Heki* [2001] and *Heki and Miyazaki* [2000].

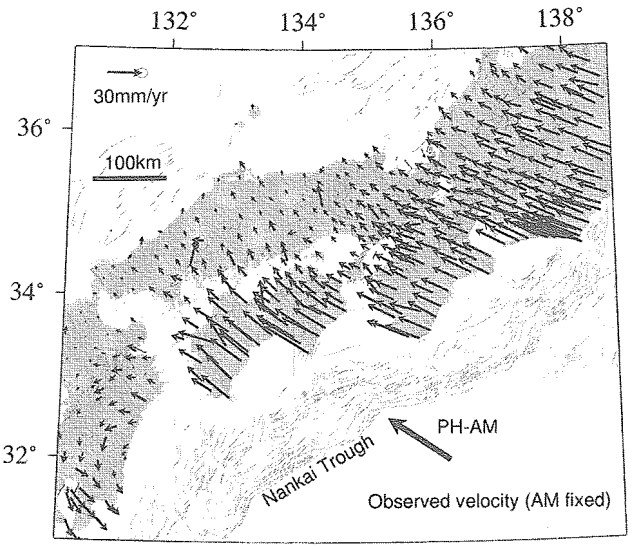

Figure 10. Crustal velocity field of southwest Japan relative to the Amurian Plate.

Figures 10 shows the velocity field of southwest Japan relative to AM. Similary to the result that is shown in the previos sections, the eastward movement in Chugoku district found in the velocity field relative to EU changed its direction to the northwestward, due to the elastic deformation by the interaction with PH. As suggested by the velocity field of Japan relative to EU [e.g. *Sagiya et al.*, 2000], it is also likely that the eastern margin of AM is affected by the collision with the northeastern Japan arc. In other words, the observed velocity field is probably a mixture of the largely elastic deformation from the interaction with PH and an elastic/non-elastic one from the interarc collision.

Separation of the observed field into two deformations was tried by *Miyazaki and Heki* [2001]. They pointed out that the collisional deformation pattern is consistent with focal mechanisms of crustal earthquakes in southwest Japan. *Heki and Miyazaki* [2000] extended their method to the Tokai district, the area where the collisional deformation is accommodated, and found that the convergence rate beneath the Tokai district is about one-third that of the Shikoku district. A clear understanding of

This document is provided by JAXA.

crustal dynamics in southwest Japan will help us determine if there is a causal relationship with the occurrence of inland earthquakes.

7 Conclusion

We analyzed GPS data from the Russian Far East, Korea, and China, together with five GEONET sites to determine the Amurian plate motion. The main conclusions are as follows:

1. The existence of the Amurian plate has been confirmed using GPS velocity data.
2. The Euler vector of the Amurian plate has been estimated. The obtained Euler vector predicts the Amurian plate movement that is consistent with geophysical and geological observations of relative plate motions along its boundary, with the exception of slip vector data from the Baikal Rift.
3. Our determination of the Amurian plate motion makes it possible to investigate the intraplate velocity field in the southwest Japan during the interseismic period.
4. The intraplate deformation in southwest Japan is characterized by interaction with the Philippine Sea plate at the Nankai Trough and interarc collision with northeast Japan.

Acknowledgements

The author, S. M., would like to express his sincere appreciation to Prof. Tomowo Hirasawa for his guidance, hearty encouragement and discussions. We are indebted to Prof. Tetsuzo Seno (University of Tokyo) for his suggestions, comments, and discussions. We also thank Dr. Nikolay F. Vasilenko, Dr. Alexei Ivashchenko (both at Institute of Marine Geology, Russian Academy of Science), Prof. Fumiaki Kimata (Nagoya University), Dr. Satoshi Miura (Tohoku University) for the establishment and maintenance of the GPS stations at Yuzhno-Sakhalinsk and OXA. The GPS station at Vladivostok is established and maintained by Prof. Teruyuki Kato (University of Tokyo)and Dr. Mikhail D. Gerasimenko (Institute of Applied Mathematics, Russia). We would also like to express our gratitude to Dr. Fyodor G. Korchagin and Dr. Margarita Lunyova (Institute of Tectonics and Geophysics) for collaborating the plans to establish GPS stations in Far East Russia and their discussion on the tectonics in that region. Although this plan has unfortunately been delayed mainly due to the international affairs, we are currently making efforts to overcome these difficulties. A software package, Generic Mapping Tool (GMT)[*Wessel and Smith*, 1995], was used to plot the figures. Part of this work was supported by Special Coordination Funds of the Science and Technology Agency of the Japanese Government.

References

[*Argus and Gordon*, 1991] Argus, D. F. and R. G. Gordon, No-net-rotation model of current plate velocities incorporating plate motion model NUVEL-1, *Geophys. Res. Lett., 18,* 2039-2042, 1991.

[*DeMets et al.*, 1990] DeMets, C., R. G. Gordon, D. F. Argus and S. Stein, Current plate motions, *Geophys. J. Int., 101,* 425-478, 1990.

[*DeMets et al.*, 1994] DeMets, C., R. G. Gordon, D. F. Argus and S. Stein, Effect of recent revisions to the geomagnetic reversal time scale on estimates of current plate motions, *Geophys. Res. Lett., 21,* 2191-2194, 1994.

[*Hashimoto et al.*, 1996] Hashimoto, M., T. Sagiya, H. Tsuji, Y. Hatanaka and T. Tada, Coseismic displacement of the 1995 Kobe earthquake, *J. Phys. Earth, 44,* 255-279, 1996

[*Heflin*, 1998] Heflin, M. B., Plate motion from Global Positioning System,
http://sideshow. jpl. nasa. gov/mbh/series. html, 1998.

[*Heki*, 1996] Heki, K., Horizontal and vertical crustal movements from three-dimensional very long baseline interferometry kinematic reference frame: Implication for the reversal time scale revision, *J. Geophys. Res., 101,* 3187-3198, 1999.

[*Heki et al.*, 1999] Heki, K., S. Miyazaki, H. Takahashi, M. Kasahara, F. Kimata, S. Mira, N. F. Vasilenko, A. Ivashchenko, and K. An, The Amurian plate motion and curent plate kinematics in eastern Asia, *J. Geophys. Res., 104,* 29, 147-29, 155, 1999.

[*Heki and Miyazaki*, 2000] Heki, K., and S. Miyazaki, Plate convergence and long-term crustal deformation in central Japan, *Geophys. Res. Lett.,* submitted, 2000.

This document is provided by JAXA.

[*Holt et al.*, 1995] Holt, W. E., M. Li and A. J. Haines, Earthquake strain rates and instantaneous relative motions within central and eastern Asia, *Geophys. J. Int., 122,* 569-593, 1995.

[*Ishibashi*, 1995] Ishibashi, K., The 1995 Kobe, Japan, earthquake (M7. 1) in the "Amurian Plate Eastern Margin Mobile Belt" and its implication to the regional seismic activity (Preliminary)(in Japanese), *Chishitsu News, 490,* 14-21, 1995.

[*Kato et al.*, 1998a] Kato, T, G. S. El-Fiky, E. N. Oware, and S. Miyazaki, Crustal strains in the Japanese islands as deduced from dense GPS array *Geophys. Res. Lett., 25,* 3445-3448, 1998.

[*Kato et al.*, 1998b] Kato, T., Y. Kotake, S. Nakao, J. Beavan, K. Hirahara, M. Okada, M. Hoshiba, O. Kamigaichi, R. B. Feir, P.-H. Park, M. D. Gerasimenko, and M. Kasahara, Initial results from WING, the continuous GPS network in the western Pacific area, *Geophys. Res. Lett., 25,* 369-372, 1998.

[*Kotake et al.*, 1998] Kotake, Y., T. Kato, S. nakao, K. Hirahara, M. Okada, O. Kamigaichi, M. Hoshiba, M. Kasahara, J. Beavan, R. B. Feir, M. D. Gerasimenko and P-H. Park, On the data analysis of the Western Pacific Integrated Network of GPS (part 1), *J. Geod. Soc. Japan, 44,* 1-19, 1998.

[*Kuge et al.*, 1996] Kuge, K., J. Zhang and M. Kikuchi, The July 12, 1993 Hokkaido-Nansei-Oki, Japan, earthquake: Effects of source complexity on surface-wave radiation, *Bull. Seism. Soc. Am., 86,* 505-518, 1996.

[*Miyazaki et al.*, 1996] Miyazaki, S., K. Heki, T. Sagiya, Y. Hatanaka and H. Tsuji, Determination of the Euler Vector between the Amurian and the Eurasian plates with GPS data (in Japanese), *Abstract of Seism. Soc. Japan, No.2,* B40, 1996.

[*Miyazaki*, 1999] Miyazaki, S, Interseismic crustal deformation in and around the Japanese Islands as deduced from GPS observations, Ph. D, thesis, 129pp, Tohoku Univ., Sendai, 1999.

[*Miyazaki and Heki*, 2001] Miyazaki, S. and K. Heki, Crustal velocity field of southwest Japan: Subduction and arc-arc collision, *J. Geophys. Res., 106,* 4305-4327, 2001

[*Molnar and Tapponnie*, 1975] Molnar, P. and P. Tapponnier, Cenozoic tectonics of Asia: Effects of a continental collision, *Science, 189,* 419-426, 1975.

[*Ozawa et al.*, 1999] Ozawa, T., T. Tabei and S. Miyazaki, Interplate coupling along the Nankai Trough off southwest Japan derived from GPS measurements, *Geophys. Res. Lett., 26,* 927-930, 1999.

[*Pacheco et al.*, 1993] Pacheco, J. F., L. R. Sykes and C. H. Scholz, Nature of seismic coupling along simple plate boundaries of the subduction type, *J. Geophys. Res., 98,* 14, 133-14, 159, 1993.

[*Peltzer et al.*, 1985] Peltzer, G., P. Tapponnier, Z. Z. Tao and X. Z. Qin, Neogene and Quaternary faulting in and along the Qin Ling Shan, *nature, 317,* 500-505, 1985.

[*Peltzer and Saucier*, 1996] Peltzer, G. and F. Saucier, Present-day kinematics of Asia derived from geologic fault rates, *J. Geophys. Res., 101,* 27, 943-27, 956, 1996.

[*Sagiya et al.*, 2000] Sagiya, T., S. Miyazaki, and T. Tada, Continuous GPS array and present-day crustal deformation of Japan, *Pure Appl. Geophys.*, 157, 2303-2322, 2000.

[*Seno et al.*, 1993] Seno, T., S. Stein and A. E. Gripp, A model for the motion of the Philippine Sea plate consistent with NUVEL-1 and geological data, *J. Geophys. Res., 98,* 17, 941-17, 948, 1993.

[*Seno et al.*, 1996] Seno, T., T. Sakurai and S. Stein, Can the Okhotsk plate be discriminated from the North American plate?, *J. Geophys. Res., 101,* 11, 305-11, 315, 1996.

[*Takahashi et al.*, 1999] Takahashi, H., M. Kasahara, F. Kimata, S. Miura, K. Heki, T. Seno, N. Vasilenko, A. Ivashchenko, V. Bahtiarov, V. Levin, E. Gordeev, F. Korchagin, and M. Gerasimenko, Velocity field of around the Sea of Okhotsk and Sea of Japan regions determined from a new continuous GPS network data, *Geophys. Res. Lett., 26,* 2533-2536, 1999.

[*Tamaki and Honza*, 1985] Tamaki, K. and E. Honza, Incipient subduction and obduction along the eastern margin of the Japan Sea, *Tectonophysics, 119,* 391-406, 1985.

[*Wei and Seno*, 1998] Wei, D.-P., and T. Seno, Determination of the Amurian plate motion, in *Mantle Dynamics and Plate Interactions in East Asia, Geodyn. Ser.*, vol. 27, edited by M. F. J. Flower et al., 419pp, AGU, Washington, D. C., 1998.

This document is provided by JAXA.

[*Wessel and Smith*, 1995] Wessel, P. and W. H. F. Smith, New version of the Generic Mapping Tools released, *EOS Trans. Am. Geophys. Union, 76,* 329, 1995.

[*Zhang et al.*, 1995] Zhang, Y. Q., P. Vergely and J. Mercier, Active faulting in and along the Qinling range (China) inferred from SPOT imagery analysis and extrusion tectonics of South China, *Tectonophysics, 243,* 69-95, 1995.

[*Zonenshain and Savostin*, 1981] Zonenshain, L. P. and L. A. Savostin, Geodynamics of the Baikal rift zone and plate tectonics of Asia, *Tectonophysics, 76,* 1-45, 1981.

This document is provided by JAXA.